Published in final edited form as:
Nat Chem Biol. 2013 September ; 9(9): 586–592. doi:10.1038/nchembio.1308.

Proteostasis of polyglutamine varies among neurons and predicts neurodegeneration

Andrey S Tsvetkov[1,2], **Montserrat Arrasate**[1,2,8], **Sami Barmada**[1], **D Michael Ando**[3], **Punita Sharma**[1,2], **Benjamin A Shaby**[4], and **Steven Finkbeiner**[1,2,3,5,6,7,*]

[1]Gladstone Institute of Neurological Disease, San Francisco, California, USA.

[2]Taube-Koret Center for Neurodegenerative Disease Research, San Francisco, California, USA.

[3]Biomedical Sciences Graduate Program, University of California–San Francisco, San Francisco, California, USA.

[4]Department of Statistical Science, Duke University, Durham, North Carolina, USA.

[5]Graduate Programs in Neuroscience and Biomedical Sciences, University of California–San Francisco, San Francisco, California, USA.

[6]Program in Biological Sciences and Medical Scientist Training Program, University of California–San Francisco, San Francisco, California, USA.

[7]Department of Neurology and Physiology, University of California–San Francisco, San Francisco, California, USA.

Abstract

In polyglutamine (polyQ) diseases, only certain neurons die, despite widespread expression of the offending protein. PolyQ expansion may induce neurodegeneration by impairing proteostasis, but protein aggregation and toxicity tend to confound conventional measurements of protein stability. Here, we used optical pulse labeling to measure effects of polyQ expansions on the mean lifetime of a fragment of huntingtin, the protein that causes Huntington's disease, in living neurons. We show that polyQ expansion reduced the mean lifetime of mutant huntingtin within a given neuron and that the mean lifetime varied among neurons, indicating differences in their capacity to clear the polypeptide. We found that neuronal longevity is predicted by the mean lifetime of huntingtin, as cortical neurons cleared mutant huntingtin faster and lived longer than striatal neurons. Thus, cell type–specific differences in turnover capacity may contribute to cellular susceptibility to toxic proteins, and efforts to bolster proteostasis in Huntington's disease, such as protein clearance, could be neuroprotective.

*sfinkbeiner@gladstone.ucsf.edu.
[8]Present address: Division of Neuroscience, Center for Applied Medical Research, University of Navarra, Pamplona, Spain.

Author contributions

A.S.T., M.A. and S.F. designed the study. A.S.T. and S.F. wrote the manuscript. B.A.S. performed statistical analysis and wrote the statistical analysis section of the manuscript. A.S.T., M.A., P.S., S.B. and D.M.A. wrote scripts for automated photoswitching and imaging. A.S.T. cloned all of the constructs used in the study. A.S.T. and M.A. cultured primary neurons and performed transfections, automated microscopy, fluorescence intensity measurements and data analysis. A.S.T. performed detergent extraction, metabolic labeling and photobleaching experiments. A.S.T. and P.S. performed survival analyses.

Competing financial interests

The authors declare no competing financial interests.

Additional information

Supplementary information is available in the online version of the paper.

A hallmark of major neurodegenerative diseases is that cell death is selective. In Huntington's disease, for example, the offending protein is expressed ubiquitously, but a subpopulation of neurons from the striatum is among the first to succumb[1]. A key unsolved mystery in the field is whether the production of toxic structures, or the capacity of the protein homeostasis system itself, varies sufficiently among subpopulations of neurons to account for this cell-type specificity. Frustratingly, the best-suited method to investigate these processes, metabolic pulse labeling, yields results that are confounded by protein aggregation and toxicity and lacks resolution to uncover cell-to-cell variation in protein homeostasis.

Neurodegenerative diseases are also characterized by abnormal accumulation of misfolded proteins[2]. We therefore wondered whether the accumulation leads to neurodegeneration. At least two perspectives, which are not mutually exclusive, are possible. The first focuses on the misfolded proteins themselves, emphasizing their ability to adopt structures as monomers or aggregates that confer potentially toxic functions and lead to neurodegeneration[3,4]. The second focuses on the limited capacity of the cell to handle misfolded proteins[5], whereby doses of misfolded protein exceeding a certain capacity trigger widespread misfolding of other metastable proteins, resulting in complex loss-of-function phenotypes that mediate neurodegeneration.

To understand how a protein's propensity to misfold and how individual cellular responses to protein misfolding relate to neurodegeneration, we examined the effect of disease-associated polyQ expansions on the mean lifetime of a fragment of huntingtin, the protein that causes Huntington's disease, at the single-cell level in living neurons. Using an optical pulse-chase method, we found that polypeptides with polyQ expansions that are not bound to an inclusion body have much shorter mean lifetimes than otherwise identical versions with shorter polyQ stretches, indicating that neurons recognize disease-associated polyQ peptides specifically and effectively target them for degradation. Clearing the polyQ-expanded polypeptide was particularly dependent on autophagy, and expression of Nrf2, a transcription factor that mediates stress responses, reduced the mean lifetime of polyQ-expanded polypeptides and increased neuronal survival. To our surprise, single-cell analysis showed that the mean lifetimes of identical polypeptides varied widely from neuron to neuron, indicating that the cellular environment in which a protein is expressed has a major role in its stability. The shorter the mean lifetime of a polyQ-expanded polypeptide in cortical and striatal neurons, the longer those neurons tended to live, suggesting that the proteostasis system is a major determinant of the vulnerability of susceptible neurons to aggregation-prone proteins. Proteostasis was also an important predictor of longevity in cerebellar neurons, which are relatively spared in Huntington's disease, though additional factors substantially contributed to their ability to resist toxicity from a mutant form of a fragment of the protein that causes Huntington's disease, huntingtin ($mHtt^{ex1}$). Therefore, we conclude that differences in turnover capacity contribute to cell susceptibility to toxic proteins, and this might help explain how the same aggregation-prone protein causes neurodegeneration in some neuronal subpopulations and spares others.

We developed a new technology that enables measurement of the mean lifetime of aggregation-prone proteins in live cells and ensures that the measurements are not confounded by cell death. We applied the technology to a model of Huntington's disease and found that neurons selectively destabilize polypeptides with disease-causing polyQ expansions. We showed that neurons selectively clear diffuse $mHtt^{ex1}$, distinguishing it from wild-type forms and targeting the mutant form for accelerated clearance. By contrast, $mHtt^{ex1}$ molecules that aggregate into inclusion bodies are cleared much more slowly[6,7], offering an explanation for how mHtt accumulates in Huntington's disease.

RESULTS

Measuring protein turnover in single cells

A cell's ability to clear a protein can be inferred from how long the protein remains in a cell after it is synthesized. Conventionally, this is determined by radioactively labeling a subset of polypeptides and observing their disappearance over time[8]. However, aggregation interferes with the protein solubilization required to measure the remaining label, and cells may die before the labeled protein is degraded. Thus, conventional approaches are poorly suited to study the clearance of misfolded proteins in neurodegenerative disease.

To measure protein clearance, we developed an optical pulse-chase method that combines the photoswitchable protein Dendra2 (ref. 9) and an automated photoswitching and imaging system[10]. Brief irradiation with short-wavelength visible light causes Dendra2 to undergo an irreversible conformational change ('photoswitch') and emit red fluorescence that can be tracked until the altered molecules are cleared.

Neurons transfected with Dendra2 revealed diffuse expression throughout the cytoplasm, and no aggregation or toxicity was detected (**Fig. 1a**). After photoswitching, red fluorescence was measured in individual neurons over a week (**Fig. 1a** and **Supplementary Results, Supplementary Fig. 1a,b**). In striatal neurons, the mean lifetime was 116 ± 20 h, consistent with the longevity of other fluorescent proteins[11]. Notably, Dendra2 degradation was independent of the starting concentration (**Fig. 1b** and **Supplementary Fig. 1c**). Photobleaching did not confound these measurements: for each 1.5-s pulse (a typical duration in our experiments), red fluorescence was reduced by only 0.12% (**Supplementary Fig. 1d,e**). Notably, some neurons with the largest starting levels of Dendra2 had shorter Dendra2 mean lifetimes than did neurons with smaller starting levels (**Fig. 1c**). In fact, the mean lifetime of the identical Dendra2 polypeptide varied three- to fourfold across the population of striatal neurons, suggesting that the proteostasis machinery in individual neurons varies substantially and is a major determinant of protein metabolism (**Fig. 1d**).

We then tested whether labeled Dendra2 correctly reports the mean lifetime of a Dendra2 fusion protein (Dendra2-CL) containing a C-terminal degron that targets it for accelerated degradation[12]. The mean lifetime of Dendra2-CL was ~20% that of Dendra2 (**Fig. 1e** and **Supplementary Fig. 1a**), confirming that clearance of the Dendra2 tag was determined by the polypeptide fused to it. Next, we compared measurements with our optical method to those obtained with conventional techniques. Striatal neurons were nucleofected with Dendra2 or Dendra2-CL, grown for 1 week, pulsed with [^{35}S]methionine and chased. Dendra2 and Dendra2-CL were co-immunoprecipitated from cell extracts with Dendra2-specific antibody (anti-Dendra2), and the remaining radioactive label was measured. Again, the mean lifetime of Dendra2-CL was 20% that of Dendra2 (**Fig. 1f,g** and **Supplementary Fig. 1f,g**), confirming that optical pulse chase is a valid and sensitive way to measure protein clearance *in situ*.

An Htt^{ex1}-Dendra2 neuron model of Huntington's disease

PolyQ expansions in several proteins cause incurable adult-onset neurodegenerative diseases[13]. Huntington's disease is the most common[14]. We measured the effect of abnormal polyQ expansion on the clearance of an N-terminal fragment of wild-type Htt^{ex1} and mHtt^{ex1} in neurons. A similar fragment is generated in Huntington's disease by aberrant splicing of mHtt mRNA[15] and proteolytic cleavage of mHtt protein[16]. Expression of Htt^{ex1} produces Huntington's disease–like features in mice[17] and recapitulates many Huntington's disease features in neurons *in vitro*[18].

Studies of polyQ expansion and protein stability in cell lines yielded conflicting results[19–23]. To determine how polyQ expansion affects mHtt stability with our optical pulse-chase technique, we fused Dendra2 to the C terminus of Htt^{ex1} with a wild-type or disease-associated polyQ expansion (>36Q). First, we used our image-acquisition platform to determine whether the wild-type Htt^{ex1}-Dendra2 or $mHtt^{ex1}$-Dendra2 in striatal neurons recapitulated Huntington's disease–relevant cellular phenotypes. Neurons with $mHtt^{ex1}$-Dendra2 had a greater risk of death than neurons expressing wild-type Htt^{ex1}-Dendra2 (**Supplementary Fig. 2a**). In some neurons, Dendra2-tagged $mHtt^{ex1}$ aggregated into detergent-resistant inclusion bodies[24–26] (**Supplementary Fig. 2b**) that were never observed with Dendra2-tagged wild-type Htt^{ex1}. Similar results were obtained with Htt fragments or Htt^{ex1} tagged with different fluorescent proteins, including GFP[6,18]. Therefore, we conclude these Dendra2-tagged Htt^{ex1} variants recapitulate the polyQ-dependent toxicity and inclusion body formation typical of Huntington's disease[27,28].

We next used optical pulse labeling to investigate the turnover of Htt^{ex1} in inclusion bodies. A $mHtt^{ex1}$ containing a stretch of 72 glutamines ($mHtt^{ex1}$-Q_{72}-Dendra2) was expressed in striatal neurons along with blue fluorescent protein as a viability and morphology marker. Transfected neurons were illuminated to photoswitch $mHtt^{ex1}$-Q_{72}-Dendra2 before visible inclusion bodies formed, and red and green fluorescence images were collected. Blue fluorescence images were collected at the end of the experiment to avoid inadvertent photoswitching (**Supplementary Fig. 2c**).

Inclusion bodies that formed after photoswitching contained red and green fluorescent $mHtt^{ex1}$-Q_{72}-Dendra2 (**Supplementary Fig. 2c**). The fluorescence intensity and size of the red components of inclusion bodies remained static, whereas those of the green structures remained the same or grew slightly (**Supplementary Fig. 2d,e**). Thus, photoswitched $mHtt^{ex1}$-Q_{72}-Dendra2 aggregates together with newly synthesized, nonphotoswitched $mHtt^{ex1}$-Q_{72}-Dendra2 to form relatively stable inclusion bodies, consistent with findings in some cell lines[29].

PolyQ expansion destabilizes mHtt

Our system offers an unprecedented opportunity to measure the mean lifetime of a protein in different pools. After measuring the turnover of $mHtt^{ex1}$ in inclusion bodies, we analyzed the mean lifetime of diffuse Htt^{ex1}. Longer polyQ stretches cause more rapid and prevalent inclusion body formation, and inclusion body formation sequesters diffuse $mHtt^{ex1}$ so that $mHtt^{ex1}$ levels become undetectable outside the inclusion body[18]. Therefore, to ensure that we could detect and measure diffuse $mHtt^{ex1}$, we transfected neurons with an $mHtt^{ex1}$ variant containing a shorter polyQ stretch (46Q) that forms inclusion bodies more slowly, allowing for increased temporal resolution of its clearance. We measured the decline of photo-switched Htt^{ex1}-Q_{25}-Dendra2 and diffuse $mHtt^{ex1}$-Q_{46}-Dendra2 in neurons that had not yet started forming inclusion bodies. To our surprise, diffuse $mHtt^{ex1}$-Q_{46}-Dendra2 had a shorter mean lifetime than Htt^{ex1}-Q_{25}-Dendra2, suggesting that neurons selectively recognize and target $mHtt^{ex1}$ for accelerated degradation (**Fig. 2a–c**). We used metabolic pulse-chase analysis to measure the mean lifetimes of endogenous, full-length wild-type Htt and mHtt in Hdh150 knock-in mice[30], which have no detectable mHtt aggregation for a short period after birth. The mean lifetimes were 92 h for wild-type Htt and 39 h for polyQ-expanded mHtt (**Fig. 2d** and **Supplementary Fig. 3a,b**). Polypeptides in both experiments differed only in the polyQ length. These results strongly suggest that disease-associated polyQ expansions selectively destabilize polypeptides.

Notably, the mean lifetimes of wild-type Htt and $mHtt^{ex1}$ varied (**Fig. 2c** and **Supplementary Fig. 3c–e**). The diversity of Htt^{ex1} mean lifetimes was not due to differences in initial levels (**Supplementary Fig. 3f**) but seemed to be an intrinsic feature of

the individual neurons themselves. As striatal cultures are heterogeneous, which may explain the diversity in proteostasis capacity, we performed similar experiments in clonal N2a neuroblastoma cells. Mean lifetimes of wild-type Htt^{ex1}-Dendra2 and $mHtt^{ex1}$-Dendra2 varied in N2a cells, suggesting that proteostasis capacity varies, even within a genetically homogeneous cell population (**Supplementary Fig. 3g**).

Proteostasis of $mHtt^{ex1}$ determines degeneration

Diffuse $mHtt^{ex1}$ levels correlate inversely with lifespan[18]. In the $mHtt^{ex1}$-Q_{46}-Dendra2 system, we found that $mHtt^{ex1}$-Q_{46}-Dendra2 levels in individual neurons similarly predict neuronal longevity with an inverse relationship (**Supplementary Fig. 4a**). We wondered whether the mean lifetime of $mHtt^{ex1}$-Q_{46}-Dendra2 has predictive value. To investigate this, we measured the mean lifetime of $mHtt^{ex1}$-Q_{46}-Dendra2 in individual striatal neurons and followed each neuron over time to detect when it died, plotting the mean lifetime of diffuse $mHtt^{ex1}$-Q_{46}-Dendra2 expression against neuronal survival time. The shorter the mean lifetime of $mHtt^{ex1}$, the longer that striatal neuron lived (**Supplementary Fig. 4b**). Notably, the prognostic significance of mean lifetime was specific to $mHtt^{ex1}$; mean lifetimes or levels of Dendra2 and Htt^{ex1}-Q_{25}-Dendra2 did not predict survival (**Supplementary Fig. 4c–f**).

Next, we sought to determine whether the mean lifetime of $mHtt^{ex1}$ predicts neurodegeneration. Diversity in the mean lifetime of identical polypeptides (**Fig. 1d** and **Supplementary Fig. 3c–e**) suggests diversity in protein homeostasis among neurons. Therefore, the prognostic value of the mean $mHtt^{ex1}$ lifetime could indicate that (i) aggregation-prone proteins induce neurodegeneration by stressing the proteostasis system, causing further stress on the folding of a subset of client proteins[5], or (ii) aggregation-prone proteins adopt toxic conformations[3,4], with aggregation strongly dependent on the concentration of misfolded protein[31].

In addition to the relationship between mean $mHtt^{ex1}$ lifetime and neuronal lifespan, we found that diffuse $mHtt^{ex1}$ levels correlated negatively with lifespan[18] (**Supplementary Fig. 4a**). We wondered which of these—the dose of aggregation-prone $mHtt^{ex1}$ in a neuron or the stress it places on the proteostasis system of the neuron (as indicated by $mHtt^{ex1}$ mean lifetime)—is a better predictor of neurodegeneration. To tease apart these two covariates, we constructed a simple Bayesian regression model that estimates the effects of levels and mean lifetimes on neuronal longevity. The mean lifetime of $mHtt^{ex1}$ was threefold more important to survival than $mHtt^{ex1}$ levels (probability >0.9999) (**Fig. 3a,b**), suggesting that the proteostasis system is the dominant determinant of susceptibility to $mHtt^{ex1}$–induced degeneration in striatal neurons.

We then took a similar approach to understand how inclusion body formation is related to protein homeostasis. On the one hand, biophysical properties of purified $mHtt^{ex1}$, such as its concentration and the length of the polyQ stretch, determine its rate of aggregation *in vitro*. On the other hand, formation of at least some types of inclusion bodies in cells depends on microtubule transport and can be affected by a network of regulatory proteins[25]. To determine whether levels of $mHtt^{ex1}$ or the state of cellular proteostasis is the more relevant determinant of inclusion body formation, we measured the mean lifetime and levels of $mHtt^{ex1}$-Q_{46}-Dendra2 in the same individual neurons and followed them until they formed inclusion bodies. The mean lifetime of $mHtt^{ex1}$-Q_{46}-Dendra2 did not correlate with inclusion body formation (**Fig. 3c**).

To quantify the contributions of the mean lifetime versus levels of $mHtt^{ex1}$ on inclusion body formation, we constructed a simple Bayesian regression model. For inclusion body formation, we found that, although the initial levels of $mHtt^{ex1}$-Q_{46}-Dendra2 were relevant,

its mean lifetime was not (**Fig. 3d**). Therefore, although the inhibition of $mHtt^{ex1}$ clearance potently stimulates inclusion body formation, and inclusion body formation reduces relative stress on the ubiquitin- proteasome system (UPS)[6], the levels of $mHtt^{ex1}$, rather than the capacity of the cell to clear $mHtt^{ex1}$, best determine whether and when an inclusion body forms[18]. The processes underlying mHtt-induced inclusion body formation and neurodegeneration have been dissociated previously, but it was unclear how dissociation was possible[28,32]. These new data show that the underlying processes governing inclusion body formation and neurodegeneration are partly different.

Nrf2 enhances proteostasis and survival

We discovered that the survival of individual neurons containing $mHtt^{ex1}$ can be predicted by the efficiency of its proteostasis system, as indicated by $mHtt^{ex1}$ mean lifetime. These findings suggest that enhancing proteostasis might lower the mean lifetime of $mHtt^{ex1}$ and improve neuronal survival. To test this prediction, we attempted to shorten the mean lifetime of $mHtt^{ex1}$-Q_{46}-Dendra2 by expressing Nrf2, a transcription factor that regulates expression of stress-response genes[33], including p62, which is useful in autophagy[34]. In these experiments, striatal neurons were transfected together with Htt^{ex1}-Q_{46}-Dendra2 and Nrf2 or an empty plasmid, and the mean lifetime of $mHtt^{ex1}$-Q_{46}-Dendra2 and the overall neuronal survival were measured in both cohorts. Indeed, Nrf2 expression shortened the mean lifetime of $mHtt^{ex1}$-Q_{46}-Dendra2 (**Fig. 4a**) and increased the survival of these neurons (**Fig. 4b**). This finding underscores that a neuron's ability to identify and clear misfolded proteins may be bolstered therapeutically to promote neuronal survival.

Inhibiting UPS or autophagy affects the mean lifetimes

We found that the individual neuron-to-neuron differences in the clearance of Htt^{ex1} are as great as the average difference between wild-type and $mHtt^{ex1}$ clearance (**Supplementary Fig. 3e**). This finding was completely unexpected and raises the possibility that neurons from different brain regions have differences in the metabolism of Htt^{ex1} that are relevant to Huntington's disease. To investigate this, we measured the mean lifetime of $mHtt^{ex1}$-Q_{25}-Dendra2 and $mHtt^{ex1}$-Q_{46}-Dendra2 in striatal and cortical neurons, which seem to be differentially susceptible to Huntington's disease–mediated pathogenesis. Remarkably, we found that, although the mean lifetime of $mHtt^{ex1}$-Q_{25}-Dendra2 in cortical neurons was not different from that in striatal neurons, the mean lifetime of $mHtt^{ex1}$-Dendra2 was shorter in cortical neurons (**Fig. 5a**).

The UPS and autophagy are the major cellular protein turnover pathways. We wondered which pathways are primarily responsible for wild-type and $mHtt^{ex1}$ degradation in striatal and cortical neurons. Investigating this problem is challenging. Substantial or complete pharmacological inhibition of the UPS or autophagy promotes the formation of inclusion bodies, reducing diffuse $mHtt^{ex1}$ to levels that make optical pulse-labeling measurements unfeasible[6]. RNAi-dependent inhibition of both systems greatly affects inclusion body formation. Therefore, we measured the mean lifetimes of Htt^{ex1}-Q_{25}-Dendra2 and Htt^{ex1}-Q_{46}-Dendra2 in striatal and cortical neurons with low concentrations of inhibitors of UPS or autophagy that minimally perturb inclusion body formation by Htt^{ex1}-Q_{46}-Dendra2 (UPS inhibitor MG132, 20 μM; autophagy inhibitor 3-methyladenine (3-MA), 2.5 mM)[6].

MG132 and 3-MA each slowed Htt^{ex1} clearance in cortical and striatal neurons. Remarkably, in both cortical and striatal neurons, Htt^{ex1}-Q_{25}-Dendra2 clearance was more sensitive to UPS inhibition, and $mHtt^{ex1}$-Q_{46}-Dendra2 clearance was more sensitive to autophagy inhibition. Remarkably, cortical neurons responded more strongly overall to UPS inhibition than did striatal neurons. We therefore conclude that neurons differentially target

Htt^{ex1} to the two major protein clearance pathways depending on the length of the polyQ expansion (**Fig. 5b,c**).

Neurons respond to $mHtt^{ex1}$ by upregulating autophagy

Previously, we showed that neurons cope with $mHtt^{ex1}$ by acutely forming inclusion bodies and, in some instances, by spontaneously clearing them[7,18]. In addition, pharmacological stimulation of autophagy in our Huntington's disease model lowered levels of $mHtt^{ex1}$ and reduced inclusion bodies by inhibiting their formation and promoting their clearance. We wondered whether the coping response to $mHtt^{ex1}$ that neurons mount might involve an upregulation of autophagy in addition to acute inclusion body formation.

To determine whether autophagy flux changes in response to $mHtt^{ex1}$, we developed a sensitive and specific optical method for measuring autophagy flux in single neurons based on the clearance of the autophagy substrate Dendra2-LC3. We transfected primary striatal neurons with Dendra2-LC3 and untagged $mHtt^{ex1}$-Q_{46}, photoswitched Dendra2-LC3 and measured the decay of red Dendra2-LC3 fluorescence. In the control experiment, neurons were transfected with Dendra2-LC3 and an empty plasmid. Neurons with $mHtt^{ex1}$-Q_{46} had accelerated flux through the autophagy pathway (**Supplementary Fig. 5a**). Moreover, those neurons in which autophagy flux was greatest tended to live the longest, consistent with the possibility that autophagy upregulation by neurons occurs specifically in response to $mHtt^{ex1}$ and that it is an effective coping mechanism to mitigate toxicity (**Supplementary Fig. 5b**). These findings lead us to conclude that autophagy is a critical clearance pathway for mHtt and may be a therapeutic target[7].

Neuron-specific proteostasis contributes to degeneration

Neurons from different brain regions showed differences in the metabolism of Htt^{ex1} that are relevant to Huntington's disease (**Fig. 5a**). We therefore wondered whether striatal neurons are more susceptible to neuronal death than cortical neurons in our model, as in Huntington's disease. With survival analysis, we found that, although both striatal and cortical neurons showed $mHtt^{ex1}$-dependent neurodegeneration, striatal neurons were more susceptible to cell death (**Fig. 6a**). This result suggests that cell type–specific differences in proteostasis are responsible for the susceptibility of certain cell types.

Striatal neurons ranged widely in their ability to manage the expanded polyQ–dependent stress, and their capacity to handle misfolded protein determined their longevity. To determine whether neuron subtype–specific proteostasis contributes to neurodegeneration and longevity we measured the mean lifetime and initial levels of $mHtt^{ex1}$-Q_{46}-Dendra2 in cortical neurons and the longevity of the same neurons. Data were then incorporated into the Bayesian regression model that we developed for assessing the effects of mean lifetime and levels of $mHtt^{ex1}$-Q_{46}-Dendra2 on striatal neuron longevity (**Fig. 6b,c**). We found that, remarkably, the proteostasis capacity of a neuron, as measured by the mean lifetime of the $mHtt^{ex1}$ reporter, was again the major determinant of longevity, independent of whether the neuron originally came from the striatum or the cortex (**Fig. 6b,c**). These experiments demonstrate that the proteostasis system in cortical neurons better recognizes and clears $mHtt^{ex1}$ than its striatal counterpart, suggesting that cell type–specific differences in proteostasis are a major contributor to the specificity of striatal neurodegeneration seen in Huntington's disease.

Both striatal and cortical neurons die in Huntington's disease. We therefore wondered how neuronal cell types not affected by the disease deal with $mHtt^{ex1}$. To investigate this question, we tested whether cultured cerebellar neurons were susceptible to $mHtt^{ex1}$-Q_{46}-Dendra2 as the cerebellum is largely spared in Huntington's disease. Compared to striatal

and cortical neurons, cerebellar neurons were the least susceptible to mHtt, mirroring the pattern of cell selectivity in Huntington's disease (**Supplementary Fig. 5a,b**). We then measured the mean lifetime of this construct with our optical pulse-chase assay. Notably, the mean lifetime of $mHtt^{ex1}$-Q_{46}-Dendra2 in cerebellar neurons was relatively short, similar to that of cortical neurons (**Supplementary Fig. 6c**).

To understand whether neuronal proteostasis predicts longevity for cerebellar neurons similarly to cortical and striatal neurons, we measured the mean lifetime and levels of $mHtt^{ex1}$-Q_{46}-Dendra2 and the survival of the same neurons and determined whether the mean lifetime of $mHtt^{ex1}$-Q_{46}-Dendra2 and its levels predict neuronal longevity (**Supplementary Fig. 6d,e**). These data were then incorporated into our Bayesian regression model. As in striatal and cortical neurons, neuronal proteostasis is a predictor of neuronal survival for cerebellar neurons and is more relevant than levels of $mHtt^{ex1}$. However, the model uncovered a key difference. When the same values for the level and lifetime of $mHtt^{ex1}$ were put into the model, the survival of cortical neurons was not different from that of striatal neurons (1.028-fold (95% confidence interval: 0.936–1.124)). By contrast, the survival of cerebellar neurons was greater (1.355-fold (95% confidence interval: 1.255–1.458)) than that predicted from the level and lifetime of $mHtt^{ex1}$ alone. These results suggest that the level and lifetime of $mHtt^{ex1}$ are sufficient to fully predict the longevity of neurons, whether they come from the striatum or the cortex, two brain regions vulnerable in Huntington's disease, with proteostasis being more relevant than the expression levels of $mHtt^{ex1}$. However, factors in addition to the lifetime and the expression levels of $mHtt^{ex1}$ contribute to the longevity of cerebellar neurons by conferring resistance to $mHtt^{ex1}$ toxicity.

DISCUSSION

Our results uncovered considerable diversity in the capacity of individual neurons to identify and clear aggregation-prone proteins, which predicts their susceptibility to cell death *in vitro* and correlates with their susceptibility *in vivo*. Notably, such neuron-specific variation in protein homeostasis of a model substrate suggests an intriguing hypothesis regarding the basis for cell specificity in neurodegenerative disease. In this scheme, cell-to-cell variation in protein homeostasis capacity contributes substantially to a given cell's susceptibility to the effects of misfolded proteins. We found that striatal neurons were more vulnerable to disease-causing polyQ $mHtt^{ex1}$—and cleared $mHtt^{ex1}$ more slowly—than cortical and cerebellar neurons. Remarkably, the protein homeostasis capacity of a neuron, as measured by the mean lifetime of the mutant polyQ reporter, was the major determinant of longevity, independent of whether the neuron was striatal or cortical. Indeed, using sophisticated statistical models, we showed that stress imposed on the cellular protein homeostasis system is a better predictor of cell susceptibility than the dose of the disease-causing protein. In cerebellar neurons, which are largely spared in Huntington's disease, mean lifetime and dose of $mHtt^{ex1}$ are important determinants of longevity, with lifetime remaining more important than the expression levels, but additional factors contributed to their longevity, conferring relative resistance to $mHtt^{ex1}$ toxicity. These findings favor a unifying model in which a major mechanism by which misfolded proteins cause neurodegeneration is through stress on cellular protein homeostasis. Although protein dyshomeostasis has been implicated as a mechanism of neurodegenerative disease, it was unclear how to reconcile this proposed mechanism with the manifest cell-type specificity characteristic of neurodegenerative diseases. Our results suggest that the effectiveness of the protein homeostasis systems of striatal, cortical and cerebellar neurons differs greatly with respect to the clearance of mHtt and sufficiently enough to explain a major component of the differences among these three types of neurons in their susceptibility to mHtt-induced degeneration.

In this study, we demonstrate that clearance of $mHtt^{ex1}$ (or proteostasis capacity) is a better predictor of neurodegeneration than absolute levels of $mHtt^{ex1}$. Recently, we also showed that the extent of binding by the monoclonal antibody 3B5H10 to a mutant polyQ stretch was a more powerful predictor of neurodegeneration than levels of mutant protein[4]. The antibody 3B5H10 binds a compact hairpin structure formed preferentially by disease-associated polyQ expansions in $mHtt^{35}$. These two observations could be integrated into a single model of pathogenesis if adopting a compact structure puts stress on the protein homeostasis capacity of the cell.

Our findings have widespread ramifications for those hoping to develop therapeutics for any of the major neurodegenerative diseases. Our previous studies showed that neurons have robust coping mechanisms that identify and clear misfolded proteins, such as autophagy, and that these mechanisms may be harnessed therapeutically[7]. Here we demonstrate that the Nrf2 pathway enhances the proteostasis capacity of neurons to lower the mean lifetime of $mHtt^{ex1}$ and, importantly, increases neuronal survival. This suggests that protein homeostasis in general and the Nrf2 pathway in particular might be valuable therapeutic targets for treating misfolded protein disorders.

METHODS

Methods and any associated references are available in the online version of the paper.

Supplementary Material

Refer to Web version on PubMed Central for supplementary material.

Acknowledgments

This work was supported by grants R01 3NS039746 and 2R01 NS045191 from the US National Institute of Neurological Disease and Stroke; grant P01 2AG022074 from the National Institute on Aging; by the Huntington's Disease Society of America (made possible with a gift from the James E. Bashaw Family); the Taube-Koret Center for Neurodegenerative disease and the Gladstone Institutes (S.F.); the Milton Wexler Award and a fellowship from the Hereditary Disease Foundation (A.S.T.); a fellowship from the Hillblom Foundation (M.A.); a fellowship from California Institute for Regenerative Medicine (P.S.), and in part by DMS-0914906 from the US National Science Foundation (B.A.S.). Gladstone Institutes received support from a US National Center for Research Resources Grant RR18928-01. We thank Y. Dabaghian, I. Kelmanson, A. Gelfand and members of the Finkbeiner laboratory for helpful discussions. The animal care facility was partly supported by a US National Institutes of Health Extramural Research Facilities Improvement Project (C06 RR018928). K. Nelson provided administrative assistance, and G.C. Howard, A.L. Lucido and S. Ordway edited the manuscript.

References

1. Han I, You Y, Kordower JH, Brady ST, Morfini GA. Differential vulnerability of neurons in Huntington's disease: the role of cell type–specific features. J. Neurochem. 2010; 113:1073–1091. [PubMed: 20236390]
2. Taylor JP, Hardy J, Fischbeck KH. Toxic proteins in neurodegenerative disease. Science. 2002; 296:1991–1995. [PubMed: 12065827]
3. Kayed R, et al. Common structure of soluble amyloid oligomers implies common mechanism of pathogenesis. Science. 2003; 300:486–489. [PubMed: 12702875]
4. Miller J, et al. Identifying polyglutamine protein species *in situ* that best predict neurodegeneration. Nat. Chem. Biol. 2011; 7:925–934. [PubMed: 22037470]
5. Gidalevitz T, Ben-Zvi A, Ho KH, Brignull HR, Morimoto RI. Progressive disruption of cellular protein folding in models of polyglutamine diseases. Science. 2006; 311:1471–1474. [PubMed: 16469881]

6. Mitra S, Tsvetkov AS, Finkbeiner S. Single neuron ubiquitin-proteasome dynamics accompanying inclusion body formation in Huntington disease. J. Biol. Chem. 2009; 284:4398–4403. [PubMed: 19074152]
7. Tsvetkov AS, et al. A small-molecule scaffold induces autophagy in primary neurons and protects against toxicity in a Huntington disease model. Proc. Natl. Acad. Sci. USA. 2010; 107:16982–16987. [PubMed: 20833817]
8. Takahashi M, Ono Y. Pulse-chase analysis of protein kinase C. Methods Mol. Biol. 2003; 233:163–170. [PubMed: 12840506]
9. Gurskaya NG, et al. Engineering of a monomeric green-to-red photoactivatable fluorescent protein induced by blue light. Nat. Biotechnol. 2006; 24:461–465. [PubMed: 16550175]
10. Arrasate M, Finkbeiner S. Automated microscope system for determining factors that predict neuronal fate. Proc. Natl. Acad. Sci. USA. 2005; 102:3840–3845. [PubMed: 15738408]
11. Leutenegger A, et al. It's cheap to be colorful. Anthozoans show a slow turnover of GFP-like proteins. FEBS J. 2007; 274:2496–2505. [PubMed: 17419724]
12. Dantuma NP, Lindsten K, Glas R, Jellne M, Masucci MG. Short-lived green fluorescent proteins for quantifying ubiquitin/proteasome-dependent proteolysis in living cells. Nat. Biotechnol. 2000; 18:538–543. [PubMed: 10802622]
13. Zoghbi HY, Orr HT. Glutamine repeats and neurodegeneration. Annu. Rev. Neurosci. 2000; 23:217–247. [PubMed: 10845064]
14. DiFiglia M. Clinical Genetics, II. Huntington's disease: from the gene to pathophysiology. Am. J. Psychiatry. 1997; 154:1046. [PubMed: 9247386]
15. Sathasivam K, et al. Aberrant splicing of HTT generates the pathogenic exon 1 protein in Huntington disease. Proc. Natl. Acad. Sci. USA. 2013; 110:2366–2370. [PubMed: 23341618]
16. Wellington CL, Hayden MR. Caspases and neurodegeneration: on the cutting edge of new therapeutic approaches. Clin. Genet. 2000; 57:1–10. [PubMed: 10733228]
17. Mangiarini L, et al. Exon 1 of the HD gene with an expanded CAG repeat is sufficient to cause a progressive neurological phenotype in transgenic mice. Cell. 1996; 87:493–506. [PubMed: 8898202]
18. Arrasate M, Mitra S, Schweitzer ES, Segal MR, Finkbeiner S. Inclusion body formation reduces levels of mutant huntingtin and the risk of neuronal death. Nature. 2004; 431:805–810. [PubMed: 15483602]
19. Persichetti F, et al. Differential expression of normal and mutant Huntington's disease gene alleles. Neurobiol. Dis. 1996; 3:183–190. [PubMed: 8980018]
20. Dyer RB, McMurray CT. Mutant protein in Huntington disease is resistant to proteolysis in affected brain. Nat. Genet. 2001; 29:270–278. [PubMed: 11600884]
21. Kaytor MD, Wilkinson KD, Warren ST. Modulating huntingtin half-life alters polyglutamine-dependent aggregate formation and cell toxicity. J. Neurochem. 2004; 89:962–973. [PubMed: 15140195]
22. Roscic A, Baldo B, Crochemore C, Marcellin D, Paganetti P. Induction of autophagy with catalytic mTOR inhibitors reduces huntingtin aggregates in a neuronal cell model. J. Neurochem. 2011; 119:398–407. [PubMed: 21854390]
23. Wu JC, et al. The regulation of N-terminal Huntingtin (Htt552) accumulation by Beclin1. Acta Pharmacol. Sin. 2012; 33:743–751. [PubMed: 22543707]
24. Kazantsev A, Preisinger E, Dranovsky A, Goldgaber D, Housman D. Insoluble detergent-resistant aggregates form between pathological and nonpathological lengths of polyglutamine in mammalian cells. Proc. Natl. Acad. Sci. USA. 1999; 96:11404–11409. [PubMed: 10500189]
25. Kopito RR. Aggresomes, inclusion bodies and protein aggregation. Trends Cell Biol. 2000; 10:524–530. [PubMed: 11121744]
26. Hartl FU, Hayer-Hartl M. Converging concepts of protein folding *in vitro* and *in vivo*. Nat. Struct. Mol. Biol. 2009; 16:574–581. [PubMed: 19491934]
27. Snell RG, et al. Relationship between trinucleotide repeat expansion and phenotypic variation in Huntington's disease. Nat. Genet. 1993; 4:393–397. [PubMed: 8401588]

28. Saudou F, Finkbeiner S, Devys D, Greenberg ME. Huntingtin acts in the nucleus to induce apoptosis but death does not correlate with the formation of intranuclear inclusions. Cell. 1998; 95:55–66. [PubMed: 9778247]
29. Matsumoto G, Kim S, Morimoto RI. Huntingtin and mutant SOD1 form aggregate structures with distinct molecular properties in human cells. J. Biol. Chem. 2006; 281:4477–4485. [PubMed: 16371362]
30. Lin CH, et al. Neurological abnormalities in a knock-in mouse model of Huntington's disease. Hum. Mol. Genet. 2001; 10:137–144. [PubMed: 11152661]
31. Colby DW, Cassady JP, Lin GC, Ingram VM, Wittrup KD. Stochastic kinetics of intracellular huntingtin aggregate formation. Nat. Chem. Biol. 2006; 2:319–323. [PubMed: 16699519]
32. Slow EJ, et al. Absence of behavioral abnormalities and neurodegeneration *in vivo* despite widespread neuronal huntingtin inclusions. Proc. Natl. Acad. Sci. USA. 2005; 102:11402–11407. [PubMed: 16076956]
33. Tsakiri, EN., et al. Proteasome dysfunction in *Drosophila* signals to an Nrf2-dependent regulatory circuit aiming to restore proteostasis and prevent premature aging.. Aging Cell. 2013. http://dx.doi.org/10.1111/acel.12111
34. Riley BE, et al. Ubiquitin accumulation in autophagy-deficient mice is dependent on the Nrf2-mediated stress response pathway: a potential role for protein aggregation in autophagic substrate selection. J. Cell Biol. 2010; 191:537–552. [PubMed: 21041446]
35. Zhang QC, et al. A compact β model of huntingtin toxicity. J. Biol. Chem. 2011; 286:8188–8196. [PubMed: 21209075]
36. Bilimoria PM, Bonni A. Cultures of cerebellar granule neurons. Cold Spring Harb. Protoc. 2008 http://dx.doi.org/10.1101/pdb.prot5107.

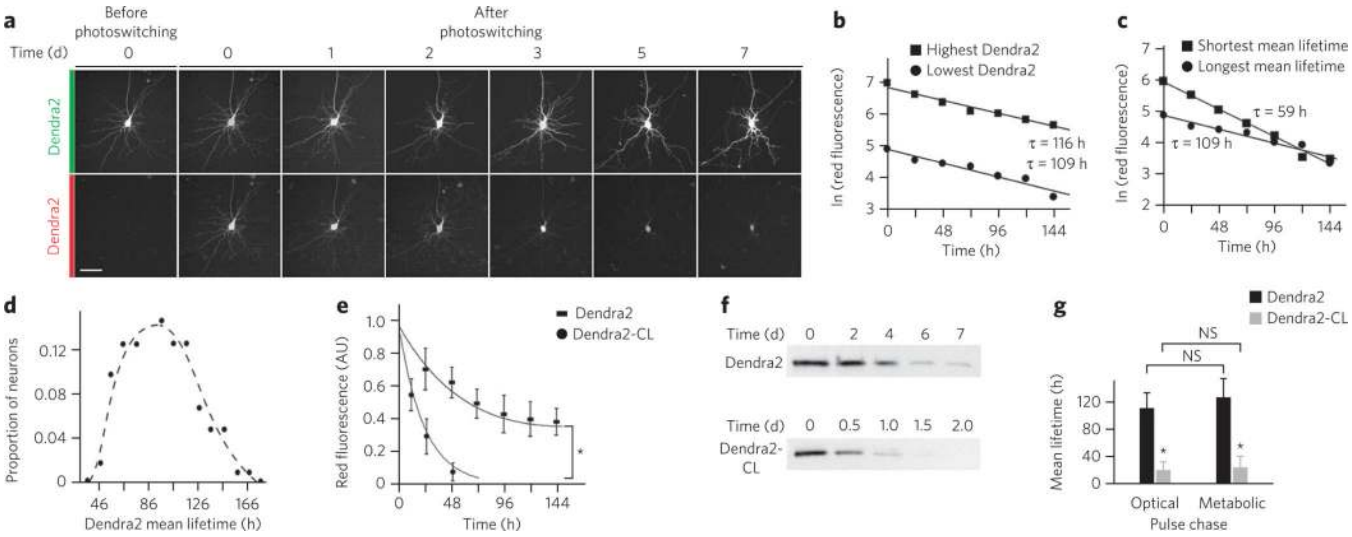

Figure 1. optical pulse labeling to measure protein turnover in individual neurons

(**a**) Optical pulse labeling of a striatal neuron expressing Dendra2 with an automated microscope. Scale bar, 50 μm. (**b,c**) The degradation of Dendra2. Neurons differing by 100-fold in starting Dendra2 expression levels had almost identical Dendra2 mean lifetimes (slopes of curves) (**b**), and some neurons with the largest starting levels of Dendra2 have shorter Dendra2 mean lifetimes than neurons with smaller starting levels. ln, natural logarithm; τ, mean lifetime. (**c**). There were three representative neurons per group. (**d**) In a cohort of striatal neurons, the mean lifetime of Dendra2 ranged three- to fourfold in a cell-specific manner. $n = 102$ neurons, analyzed from a total of three experiments. (**e**) Analysis and quantification of the decline of red fluorescence due to clearance of photoswitched Dendra2 and Dendra2-Cl (destabilized by fusion to a degron) in primary striatal neurons. AU, arbitrary units. $^*P < 0.0001$ (Student's *t*-test, log-Gaussian generalized linear model); $n = 160$ neurons, analyzed from a total of three experiments. (**f**) Striatal neurons were nucleofected with Dendra2 or Dendra2-Cl and subjected to metabolic pulse-chase analysis. Note differences in scale. (**g**) Mean lifetimes of Dendra2 and Dendra2-Cl calculated with a conventional metabolic method (gray bars) and the optical pulse-label method (black bars). Data represent mean ± s.d of three experiments; $^*P < 0.001$ (*t*-test). NS, not significant.

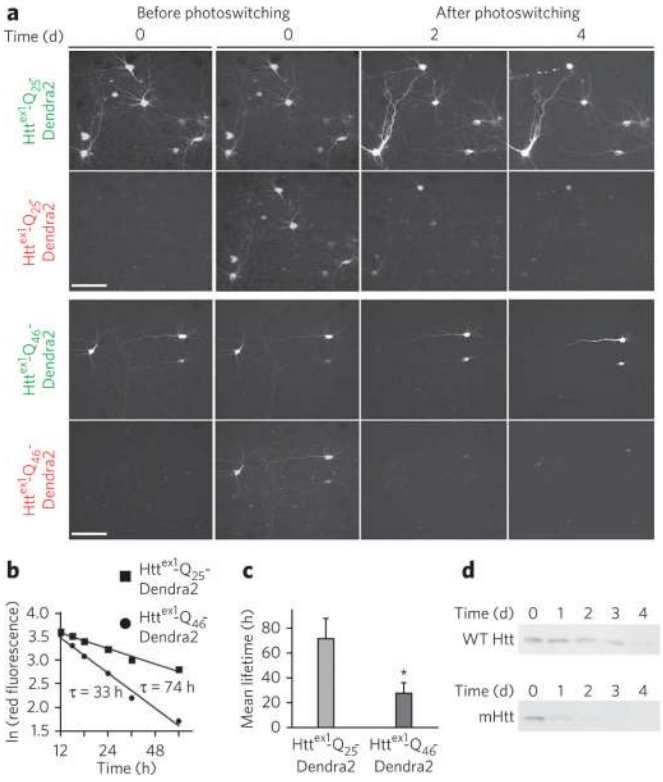

Figure 2. PolyQ expansion destabilizes diffuse mHtt^{ex1} and full-length Htt

(**a**) Automated optical pulse label of striatal neurons expressing wild-type (WT) or disease-associated Htt^{ex1} polyQ stretches. Scale bars, 50 μm. (**b**) Clearance curves of red fluorescence emitted by photoswitched mHtt^{ex1}-Q$_{25}$-Dendra2 and mHtt^{ex1}-Q$_{46}$-Dendra2. Diffuse mHtt has a shortened mean lifetime, as shown by decay of red fluorescence. There were three representative neurons per group. (**c**) Mean lifetimes of wild-type Htt^{ex1} and mHtt^{ex1} vary between neurons. $P < 0.001$ (Student's *t*-test); data represent mean ± s.d. (**Supplementary Fig. 2a–c**); $n > 100$ striatal neurons analyzed from three independent experiments. Neurons that formed inclusion bodies during the experiment were excluded from analysis. (**d**) PolyQ expansion shortens the mean lifetime of Htt in neurons. Previous work showed no detectable aggregation of mHtt in embryonic forebrain neurons from Hdh150 knock-in mice during a short window after birth. Homozygous mutant and wild-type cultures were subjected to metabolic labeling and pulse-chase analysis. The more rapid disappearance of mutant relative to wild-type Htt indicates that mHtt has a shorter mean lifetime. The mean lifetimes (92 h for wild-type Htt and 39 h for mHtt) are averages from two experiments.

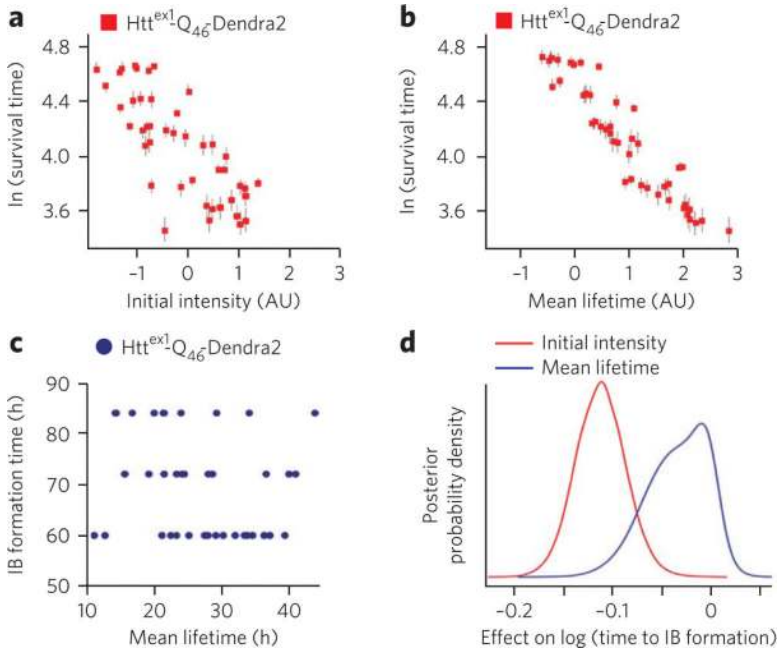

Figure 3. Proteostasis of mhtt^{ex1} determines degeneration

(**a**) Neuronal longevity correlates negatively with the fluorescence intensity of mHtt^{ex1}-Q$_{46}$-Dendra2 (or levels of diffuse mHtt^{ex1}-Q$_{46}$-Dendra2). Intensities are in standardized units (online Methods). n = 45 striatal neurons, analyzed from three independent experiments. (**b**) The proteostasis capacity of a striatal neuron to destabilize and clear mHtt^{ex1}, as inferred from the mean lifetime of mHtt^{ex1}, has a larger effect on survival than levels of mHtt^{ex1} (as shown in **a**) (that is, shorter mean lifetimes are associated with long-living neurons). Mean lifetimes are in standardized units (online Methods). n = 45 striatal neurons, analyzed from three independent experiments. (**c,d**) Initial levels but not mean lifetime of mHtt^{ex1}-Q$_{46}$-Dendra2 predict inclusion body formation. Inclusion body formation was analyzed to investigate the relationship in single neurons between initial levels or mean lifetime of mHtt^{ex1}-Q$_{46}$-Dendra2 and the time point when an inclusion body forms. (**c**) The mean lifetime of Htt^{ex1}-Q$_{46}$-Dendra2 does not correlate with the time point of inclusion body formation. R^2 = 0.04. (**d**) To investigate the relative contribution of initial levels or mean lifetime of diffuse Htt^{ex1}-Q$_{46}$-Dendra2 to the timing of inclusion body formation in neurons, a Bayesian model was constructed. The probability density for the mean lifetime of diffuse Htt^{ex1}-Q$_{46}$-Dendra2 is clustered around '0', indicating that the mean lifetime of Htt^{ex1}-Q$_{46}$-Dendra2 has little predictive value for the timing of inclusion body formation. By contrast, the probability density for the initial levels of Htt^{ex1}-Q$_{46}$-Dendra2 in relation to the timing of inclusion body formation is shifted leftward, indicating that the larger the level of Htt^{ex1}-Q$_{46}$-Dendra2, the sooner inclusion body formation occurs. n = 37 neurons, analyzed from three independent experiments.

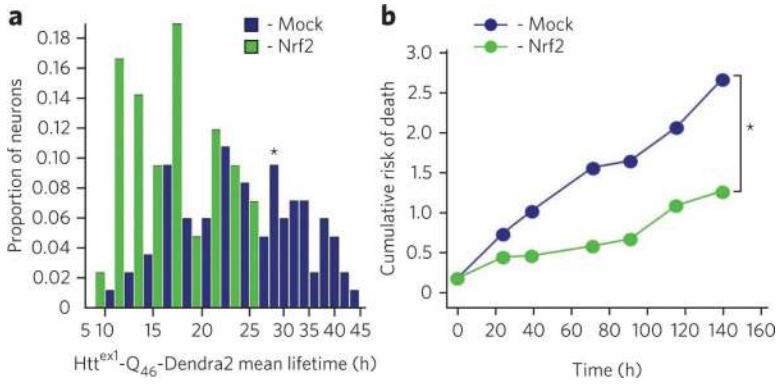

Figure 4. Nrf2, a stress-activated transcription factor, shortens the mean lifetime of mHtt^{ex1}-Q$_{46}$-Dendra2 and increases survival of striatal neurons

Striatal neurons were transfected with Htt^{ex1}-Q$_{46}$-Dendra2 and Nrf2 or an empty control vector. The mean lifetime of Htt^{ex1}-Q$_{46}$-Dendra2 and survival were determined for individual neurons. (**a**) Nrf2 significantly shifted the distribution of mean lifetimes of mHtt^{ex1}-Q$_{46}$-Dendra2 to lower values compared to empty vector control, indicating Nrf2-accelerated mHtt clearance. *P = 0.0004 (Wilcoxon test; median values are 24.8 h for Htt^{ex1}-Q$_{46}$-Dendra2 plus mock and 19.4 h for Htt^{ex1}-Q$_{46}$-Dendra2 plus Nrf2). n = 82 neurons. (**b**) Nrf2 significantly decreased the cumulative risk of death in striatal neurons with mHtt^{ex1}-Q$_{46}$-Dendra2 compared to empty vector control. *P < 0.001 (Mantel-Cox test). n = 307 neurons.

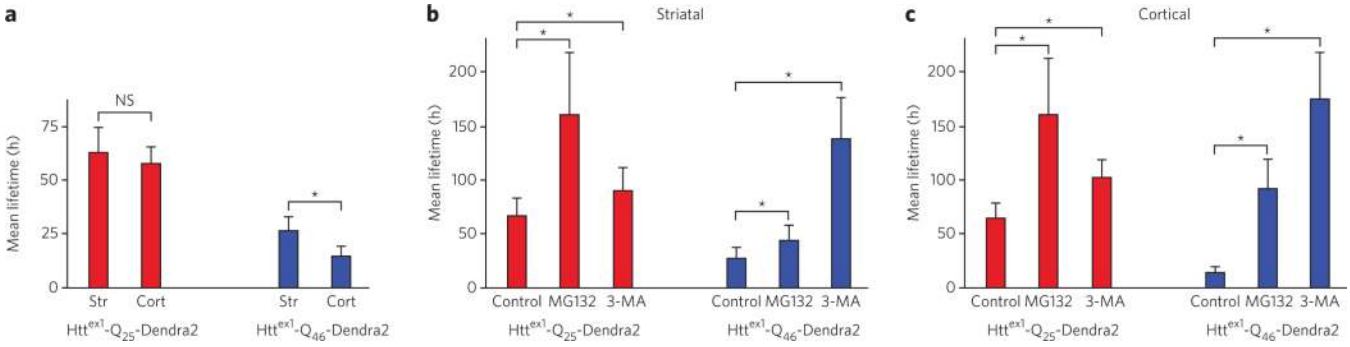

Figure 5. Inhibiting the ubiquitin-proteasome system or autophagy differentially affects the mean lifetimes of Htt^{ex1}-Q$_{25}$-Dendra2 and mHtt^{ex1}-Q$_{46}$-Dendra2

(**a**) Cultured striatal (Str) and cortical (Cort) neurons were transfected with Htt^{ex1}-Q$_{25}$-Dendra2 and mHtt^{ex1}-Q$_{46}$-Dendra2 and then subjected to photoswitching, and the mean lifetimes of Htt^{ex1}-Q$_{25}$-Dendra2 and mHtt^{ex1}-Q$_{46}$-Dendra2 were measured. $P < 0.001$ (Student's *t*-test; data represent mean ± s.d.); $n = 152$ neurons. (**b**) Cultured striatal neurons were transfected with Htt^{ex1}-Q$_{25}$-Dendra2 and mHtt^{ex1}-Q$_{46}$-Dendra2 and then subjected to photoswitching. Cells were left untreated (control) or treated with the UPS inhibitor MG132 (20 μM) or the macroautophagy inhibitor 3-MA (2.5 mM), and the mean lifetimes of Htt^{ex1}-Q$_{25}$-Dendra2 and mHtt^{ex1}-Q$_{46}$-Dendra2 were measured. MG132 had a greater effect on the mean lifetime of Htt^{ex1}-Q$_{25}$-Dendra2 than 3-MA, whereas 3-MA had a greater effect on Htt^{ex1}-Q$_{46}$-Dendra2 than MG132. $P < 0.01$ (analysis of variance); data represent mean ± s.d.; $n = 60$ neurons. (**c**) Cultured cortical neurons were transfected with Htt^{ex1}-Q$_{25}$-Dendra2 and mHtt^{ex1}-Q$_{46}$-Dendra2 and then subjected to photoswitching. Cells were left untreated (control) or treated with the UPS inhibitor MG132 (20 μM) or the macroautophagy inhibitor 3-MA (2.5 mM), and the mean lifetimes of Htt^{ex1}-Q$_{25}$-Dendra2 and mHtt^{ex1}-Q$_{46}$-Dendra2 were measured. MG132 had a greater effect on the mean lifetime of Htt^{ex1}-Q$_{25}$-Dendra2 than 3-MA, whereas 3-MA had a greater effect on Htt^{ex1}-Q$_{46}$-Dendra2 than MG132. $P < 0.01$ (analysis of variance); data represent mean ± s.d.; $n = 60$ neurons.

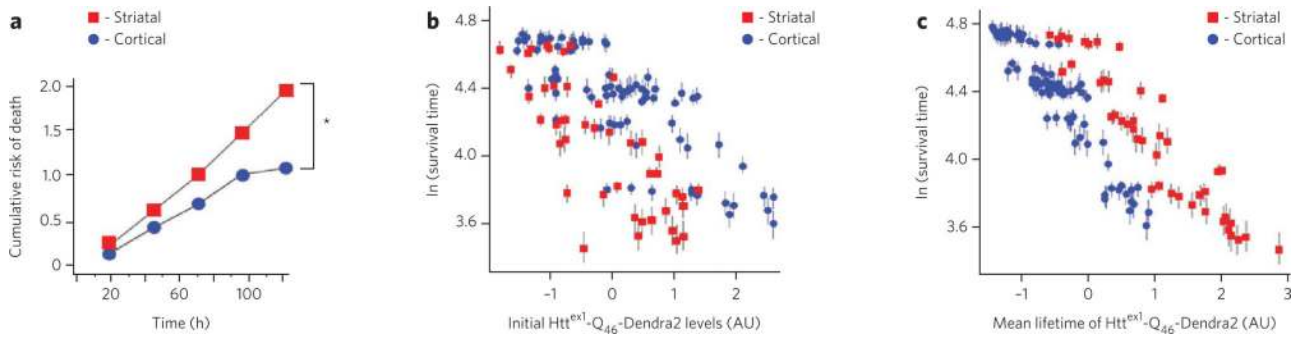

Figure 6. Neuron type–specific proteostasis of mHtt^{ex1} contributes to their susceptibility to degeneration

(**a**) Hazard analysis shows that Dendra2-tagged mHtt^{ex1} (Htt^{ex1}-Q$_{46}$-Dendra2) increases the risk of death for striatal neurons more than it does for cortical neurons. Neurons that formed inclusion bodies during the experiment were excluded. $P < 0.001$ (Mantel-Cox test); $n = 100$ neurons analyzed per group. (**b**) Neuronal longevity correlates negatively with the fluorescence intensity of mHtt^{ex1}-Q$_{46}$-Dendra2 (or levels of diffuse mHtt^{ex1}-Q$_{46}$-Dendra2). Intensity values are in standardized units. $n = 85$ striatal and $n = 50$ cortical neurons. (**c**) The proteostasis capacity of a neuron (striatal or cortical) to destabilize and clear mHtt^{ex1}, as inferred from the mean lifetime of the mHtt^{ex1} it contains, has a larger effect on survival than level of mHtt^{ex1} (as shown in **b**) (that is, shorter mean lifetimes are associated with long-living neurons) in striatal and cortical neurons. Mean lifetimes are in standardized units; $n = 85$ striatal neurons and $n = 50$ cortical neurons.